YOUR TITLE HERE

A Dissertation

By

HABARAKADA LIYANAGE ANUSHA PUSHPAKUMARI

Submitted to the Graduate College of Hampton University in
partial fulfillment of the requirements for the degree of

DOCTOR OF PHILOSOPHY

August 2013

This dissertation submitted by Habarakada Liyanage Anusha Pushpakumari in partial fulfillment of the requirements for the degree of Doctor of Philosophy at Hampton University, Hampton, Virginia is hereby approved by the committee under whom the work has been completed.

Michael Kohl, Ph.D.
Committee Chair

M. Eric Christy, Ph.D.

Jose L. Goity, Ph.D.

Mark Jones, Ph.D.

Patrena N. Benton, Ph.D.
Dean, The Graduate College

Date

ABSTRACT

Your Title Here. (August 2013)

Habarakada Liyanage Anusha Pushpakumari, B.S., University of Peradeniya;

M.S., Hampton University

Chair of Advisory Committee: Dr. Michael Kohl

Lots of abstract stuff here.

Dedicated to my parents.

ACKNOWLEDGEMENTS

I would like to acknowledge ...

TABLE OF CONTENTS

Section Page

LIST OF TABLES

Table Page

LIST OF FIGURES

SECTION 1

INTRODUCTION

Since Rutherford, Geiger, and Marsden discovered the atomic nucleus by measuring the distribution of alpha particles scattered from gold foils ([1–3]), scientists started to believe that the nucleus consists of a dense center surrounded by a cloud of negatively charged electrons. These electrons are bound to the nucleus by the electromagnetic force which causes the interaction between electrically charged particles.

The nucleus consists of nucleons, *i.e.*, protons and neutrons, which themselves have a substructure. The effort of understanding the nucleonic structure and dynamics has continued for generations up to this day. The first clue that the nucleons themselves are not point-like, elementary particles came from Otto Stern's measurements of the magnetic moment of the proton and the deuteron in 1933 [4]. These measurements showed drastic deviation from the expected value in the Dirac equation for a "point" spin 1/2 particle, implying that protons and neutrons are composite and have internal structure. Since that groundbreaking discovery, a modern understanding of the nucleon has emerged, answering many questions and raising many more.

Elastic electron-nucleon scattering has been an important tool to understand the structure of the nucleon. In one-photon exchange (Born) approximation, the structure of the nucleon is characterized in terms of the electric and magnetic form factors, G_E and G_M, which depend only on the four-momentum transfer squared, Q^2. The form factors, G_E and G_M, are fundamental quantities sensitive to the distribution of charge and magnetization within the nucleon.

The proton form factors, G_E^p and G_M^p, can be extracted individually by measuring the elastic ep scattering cross-sections at constant Q^2, but at different beam energies

and at the different electron scattering angles (Rosenbluth technique). In addition, spin observables in elastic *ep* scattering are sensitive to the ratio of G_E^p/G_M^p, allowing for a direct determination of G_E^p/G_M^p from either the recoil-polarization measurement or the double-spin asymmetry at a single beam energy and a single electron scattering angle. A linear falloff with Q^2 was shown in the polarization-transfer data in contrast to the nearly flat Q^2 dependence of G_E^p/G_M^p measured with the Rosenbluth technique. This discrepancy has been widely considered as due to the significant effects of two-photon exchange. Checking for the possibility of an unknown systematic error in the Rosenbluth or recoil-polarization technique is very important, before physical conclusions can be made. Measurement of the beam-target asymmetry in elastic *ep* scattering offers an independent technique of determining the G_E^p/G_M^p ratio. By measuring G_E^p/G_M^p with the third technique and comparing to previous results, the discovery of unknown or underestimated systematic errors in the previous measurements is possible. This dissertation presents the measurement of G_E^p/G_M^p from double-spin asymmetry for $Q^2 = 2.06$ (GeV/c)^2 and 5.66 (GeV/c)^2.

1.1 Overview of the Experiment

The experiment E07-003 (Spin Asymmetries of the Nucleon Experiment) is a single-arm inclusive-scattering experiment. The goal of SANE was to measure proton spin structure functions $g_1(x, Q^2)$ and $g_2(x, Q^2)$ at four-momentum transfer $2.5<Q^2<6.5$ (GeV/c)^2 and $0.3<x<0.8$ which is an extension of the kinematics of experiment RSS [**?**] performed in Hall C, Jefferson Lab in 2007.

SANE measured the inclusive spin asymmetries with the target spin aligned parallel and nearly perpendicular (80°) to the beam direction for longitudinally polarized electron scattering from a DNP polarized proton (crystallized NH_3) target. The experiment was carried out in the experimental Hall C at Jefferson Lab from January to March, 2009. A subset of the data was used to measure the elastic beam-target spin

asymmetry from elastic electron-proton scattering. Polarized electrons with energies 4.72 GeV and 5.89 GeV were scattered from the polarized proton target with the spin of the proton aligned nearly perpendicular (80°) to the beam direction. Single-arm electron scattering data were taken by detecting the elastically scattered electrons in the High-Momentum Spectrometer (HMS) for an electron beam energy 5.89 GeV. In addition to that, recoiled protons were detected by the HMS in coincidence with the electrons in Big Electron Telescope Array (BETA) for the two different beam energies 4.72 GeV and 5.89 GeV.

Single-arm data were taken about ∼12 hours in total ($\sim 2 \times 10^4$ elastic events) and the coincidence data were taken about a week for both beam energies, ∼40 hours and ∼155 hours (∼113 elastic events and ∼1200 elastic events) respectively, for the two beam energies 4.72 GeV and 5.89 GeV.

When HMS was at negative polarity, both the HMS Cherenkov detector and the lead-glass calorimeter were used to separate pions and electrons. A relative momentum acceptance cut also was used to extract the elastic events in single-arm data.

For the coincidence data, for HMS is in positive polarity, the relative momentum deviation of the measured proton momentum in HMS from the calculated proton momentum by knowing the recoiled proton angle in HMS, was used to extract the elastic events. The vertical and horizontal positions of the scattered electron on the BETA calorimeter, BigCal was predicted from the proton angle in HMS (X_{HMS}, Y_{HMS}). By taking the horizontal and vertical position differences between the measured electron position on BigCal (X_{clust}, Y_{clust}) and the predicted electron position on BigCal (X_{HMS}, Y_{HMS}) and performing the elliptical cut on them, subtract the inelastic background most effectively.

The following Section 1.2 of the first chapter in this dissertation motivates the use of elastic electron-nucleon scattering to study the structure of the nucleon. Working in both one-photon (Born approximation) and two-photon exchange, the scattering

cross-sections are derived in terms of electric (G_E) and magnetic (G_M) form factors which characterize the effect of the nucleon's electromagnetic structure. Further, the radiative effects on the Born cross-sections is also discussed. The cross-section formula for the inelastic electron-proton scattering is also presented for the completeness of the scattering experiments.

In Chapter 2, the formalism and the methods of measuring the electromagnetic form factor ratio, $\mu G_E/G_M$ from the Rosenbluth separation technique, the polarization-transfer method and the double-spin asymmetry in terms of G_E and G_M are discussed. Existing proton and neutron form factor data from cross-section and polarization experiments are presented and discussed. In addition, possible theoretical interpretations of the nucleon electromagnetic form factors are summarized in Section **??**.

In Chapter 3, a detailed description of the experiment setup is given, including the polarized electron beam, BETA calorimeter (BigCal), HMS detector package, polarized target, trigger and data-acquisition system.

In the fourth Chapter, the data analysis is reviewed by discussing the HMS event reconstruction through the target magnetic field, HMS and BigCal detector calibrations, elastic event selections, raw and physics asymmetries and hence the proton form factor ratio, $\mu_p G_E^p/G_M^p$ calculation. The results of Montecarlo simulation comparisons of C and NH_3 data to correct the beam-position offsets and correlation corrections are also shown. In addition, the systematic uncertainty determinations for the single-arm data are discussed.

The last Chapter presents the results for the proton form factor ratio from double-spin asymmetry at two Q^2 values, $Q^2 = 2.06$ $(\mathrm{GeV/c})^2$ (with both statistical and systematic uncertainties) and 5.66 $(\mathrm{GeV/c})^2$ (with only statistical uncertainty) highliting the importance of the double-spin asymmetry method. The low HMS drift chamber efficiency of $\sim$40% due to the drift chamber gas leak during the coincidence data-taking decreased the proton yield in HMS, resulting in low statistics for the

coincidence elastic events. Therefore, due to the large error bar on the statistical uncertainty of the form factor measurement from coincidence data, the systematic uncertainty for that measurement was not studied, as it is expected not to dominate the error. Further, the possible improvements of the experiment for future references are also discussed.

1.2 Scattering Experiments

Scattering experiments have been the method of choice of nuclear and particle physicists to examine the microscopic structure of matter. To this day, electron scattering remains one of the most powerful techniques to study nuclear and nucleon structure. The interaction of a beam of electrons with a nuclear target is well understood and precisely calculable within Quantum Electrodynamics (QED). The electromagnetic fine structure constant α, the weak coupling constants g_w and g_z are all sufficiently small at all energies. However, the strong coupling constant α_s is small only at high energy in the limit of asymptotic freedom, leaving the possibility to use perturbation theory to carry out calculations of particle decay rates and scattering cross-sections. At low energies, the probed distance is larger and therefore, the strong force between quarks is stronger; QCD is non-perturbative. At higher energies, the probed distance is small; this is where the quarks are asymptotically free, the force between quarks becomes weak, and perturbative QCD applies. Starting from 'Fermi's Golden Rule', which is a general expression giving the transition rate (number of transmissions per unit time) from an initial state $\mid i\rangle$ of energy E_i to the set of final states $\mid f\rangle$ with energies $E_f = E_i$, the *invariant amplitude* or so-called *Lorentz Invariant Matrix Element*, M and hence the differential cross-section $d\sigma$ for the scattering, is derived in [5] as,

$$d\sigma = \frac{\mid \bar{M} \mid^2}{64\pi^2 M E_1} \frac{d^3p'}{p'^0} \frac{d^3k'}{k'^0} \delta^{(4)}(k + p - k' - p'), \tag{1.2.1}$$

where k, p and k', p' are the initial and final particle four-momenta. The bar over the square of the scattering amplitude indicates that it is to be averaged over the spin states of the initial particles and summed over the spin states of the outgoing particles. Therefore, in other words, the Equation (1.2.1) refers to the *unpolarized* cross-section.

By integrating over all possible outgoing momenta, assuming the two-body scattering process of the form $1 + 2 \rightarrow 3 + 4$, the above Equation (1.2.1) converts to the differential cross-section describing the scattering of a particle into an element of solid angle, $d\Omega$ in the lab frame,

$$\frac{d\sigma}{d\Omega} = \frac{1}{64\pi^2}\left(\frac{E_3}{ME_1}\right)^2 \mid \bar{M} \mid^2, \tag{1.2.2}$$

where E_1 and E_3 are the energies of the incoming and scattered particle, respectively. Note that $d\Omega = 2\pi \mathrm{d}\cos\theta$. The above expression for the differential cross-section depends on the Lorentz-invariant matrix element squared, $\mid \bar{M} \mid^2$, which contains the dynamical information on the process. The matrix element is determined by Feynman diagrams appropriate to that process and applying the Feynman rules (See [6], section 4.8 or [5], table 6.2) to each diagram.

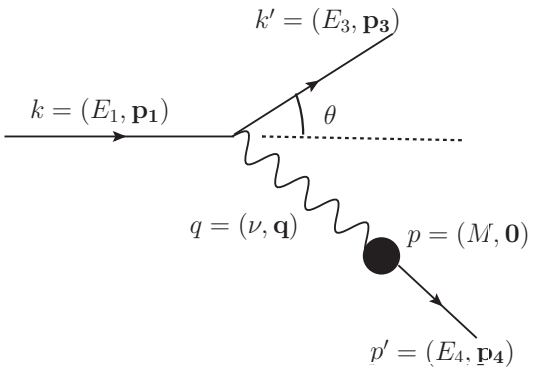

Figure 1.1. Lab frame electron scattering from a stationary target.

Figure 1.1 shows the most basic scattering process, elastic lepton - lepton scattering. At leading order in α, the scattering occurs through the exchange of a single virtual photon. Because the fine structure constant of electromagnetism is so small ($\alpha = \frac{e^2}{\hbar c}$ (in cgs units)= $\frac{1}{137.03599911}$ experimentally [7]), first-order perturbation theory in α (Born approximation) is a very good approximation to the real physics process.

According to the Feynman rules for QED, the invariant amplitude for lepton-lepton scattering can be read off from the diagram as,

$$-iM = \bar{u}(k')(ig_e\gamma^\mu)u(k)\left(-i\frac{g_{\mu\nu}}{q^2}\right)\bar{u}(p')(-ig_e\gamma^\nu)u(p). \tag{1.2.3}$$

In Equation (1.2.3), $u(k)$ and $\bar{u}(k')$ are the solutions to the momentum space Dirac equation $(\gamma^\mu p_\mu - mc)u = 0$ for incoming and outgoing particles. The quantity $q^2 = (k-k')^2 = (p'-p)^2$ is the four-momentum transfer squared and also the invariant mass of the virtual photon. Each vertex adds a vertex factor, $ig_e\gamma^\mu$, with g_e representing the coupling strength of the vertex, here the charge of the electron, $g_e = e$. The photon propagator, $-i\frac{g_{\mu\nu}}{q^2}$ is sandwiched between them. Squaring the invariant amplitude $-iM$, one can obtain:

$$\mid M \mid^2 = \frac{e^4}{(k-k')^2}[\bar{u}(k')\gamma^\mu u(k)][\bar{u}(p')\gamma_\nu u(p)][\bar{u}(k')\gamma^\mu u(k)]^*[\bar{u}(p')\gamma^\nu u(p)]^*. \tag{1.2.4}$$

However, because of the lack of knowledge of the spin degrees of freedom, the average of the all-spin states of $\mid M \mid^2$, $\mid \bar{M} \mid^2$ was calculated by averaging over initial spins and summing over final spins to find the *unpolarized* scattering amplitude of the process. In parallel, the invariant amplitude square, $\mid \bar{M} \mid^2$ for lepton-nucleon scattering can be written in different form as,

$$|\bar{M}|^2 = \frac{e^4}{q^4}L_e^{\mu\nu}L_{\mu\nu}^{target}, \tag{1.2.5}$$

introducing the new quantities L, which are the leptonic and hadronic tensors. The leptonic tensor expression is defined in [5] as:

$$L_e^{\mu\nu} = \frac{1}{2}Tr((\not{k}' + m)\gamma^\mu(\not{k} + m)\gamma^\nu) = 2(k'^\mu k^\nu + k'^\nu k^\mu - (k'.k - m^2)g^{\mu\nu}), \quad (1.2.6)$$

which gives information about the lepton arm of the scattering process. The hadronic tensor, $L_{\mu\nu}^{target}$ gives information about the hadron arm of the scattering process which is particular to each nucleon type. However, for lepton-lepton scattering, the hadronic tensor in Equation (1.2.5) should be replaced by the leptonic tensor which is given by Equation (1.2.6). Therefore, by substituting the leptonic tensor, Equation (1.2.6) for both $L_e^{\mu\nu}$ and $L_{\mu\nu}^{target}$ in Equation (1.2.5), and then using the resulting $|\bar{M}|^2$ into Equation (1.2.2), one can calculate the *unpolarized* cross-section of the lepton-lepton scattering.

Similarly, using elastic scattering of a lepton from a point-like spin-1/2, Dirac particle, one can demonstrate the cross-section calculation through the Lorentz invariant matrix element, M. By replacing the $L_{\mu\nu}^{target}$ by the Dirac particle tensor, which is assumed similar to the electron tensor, the following general expression for $\langle \mid \bar{M} \mid^2 \rangle$ is obtained for scattering of e^- of mass m from a Dirac particle of mass M:

$$\langle \mid \bar{M} \mid^2 \rangle = \frac{8e^4}{(k-k')^4}[(k.p)(k'.p')+(k.p')(p.k')-(k.k')M^2-(p.p')m^2+2m^2M^2]. \quad (1.2.7)$$

In the high-energy limit $k \gg m$, the electron mass can effectively be neglected. With the target particle at rest, and using energy-momentum conservation, $k+p = k'+p'$, the invariant matrix element in Equation (1.2.7) can be simplified as,

$$\langle \mid \bar{M} \mid^2 \rangle = \frac{e^4M^2}{E_1E_3\sin^4\theta/2}\left(\cos^2\theta/2 - \frac{q^2}{2M^2}\sin^2\theta/2\right), \quad (1.2.8)$$

and hence the differential cross-section from Equation (1.2.2) can be written as,

$$\frac{d\sigma}{d\Omega} = \frac{\alpha^2}{4E_1^2 \sin^4\theta/2}\frac{E_3}{E_1}\left(\cos^2\theta/2 - \frac{q^2}{2M^2}\sin^2\theta/2\right), \tag{1.2.9}$$

where $\alpha = e^2/\hbar c \approx 1/137$ is the fine structure constant. For the elastic scattering, the quantities E_3 and q^2 are given by,

$$\frac{E_3}{E_1} = \frac{M}{M + E_1(1-\cos\theta)}, \qquad q^2 = -\frac{2ME_1^2(1-\cos\theta)}{M + E_1(1-\cos\theta)} \tag{1.2.10}$$

so that the cross-section depends on only a single independent variable, θ. This seems to be the product of Rutherford-like scattering cross-section with some additional factors. The ratio E_3/E_1 gets close to unity at small scattering angles ($\theta \to 0$) where the target recoil is small. It becomes smaller as θ increases, falling to $E_3/E_1 \approx M/2E_1$ at large scattering angles, $\theta \to \pi$, where the target recoil is a maximum.

The cross-section of Equation (1.2.9) represents electron scattering from a point-like, spin-1/2, Dirac particle. Such a particle would have an intrinsic magnetic moment of magnitude, $\mu = e\hbar/(2Mc)$, *i.e.*, $\mu = 1$ in units of the nuclear magneton $\mu_N = e\hbar/(2Mc)$. If the spin-1/2 target particle is replaced by a spin 0 target particle, the $\sin^2\theta/2$ term in Equation (1.2.9) gets omitted and the cross-section becomes,

$$\left(\frac{d\sigma}{d\Omega}\right)_{Mott} = \frac{\alpha^2}{4E_1^2 \sin^4\theta/2}\frac{E_3}{E_1}\cos^2\theta/2, \tag{1.2.11}$$

known as the *Mott cross-section* with the additional recoil factor E_3/E_1. Since the spin 0 particle has no intrinsic magnetic dipole moment, the $\sin^2\theta/2$ term in Equation (1.2.9) must be due to scattering from the intrinsic magnetic dipole moment of the spin-1/2 target particle. The $\cos^2\theta/2$ term, common to both Equations (1.2.9) and (1.2.11), must be due to scattering from the Dirac particle electric charge.

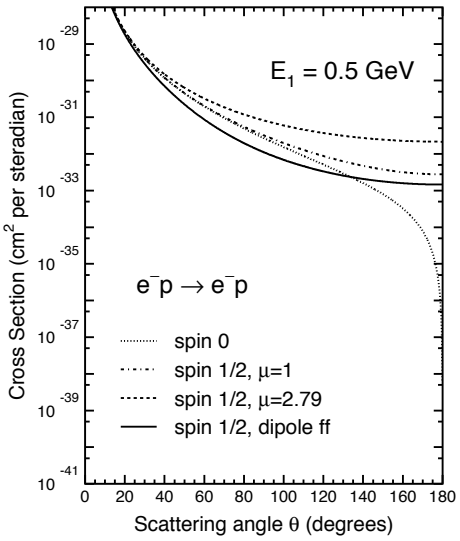

Figure 1.2. Differential cross-section $d\sigma/d\Omega$ for elastic $e^{-}p$ scattering in the lab frame, for electron beam energy of 0.5 GeV, for various assumptions about the spin and structure of the target proton [8].

Examples of the cross-sections $d\sigma/d\Omega$ and $d\sigma/d\Omega_{spin0}$ predicted by Equations (1.2.9) and (1.2.11) for a point-like Dirac target and a point-like spin-0 target are shown in Figure 1.2. For small scattering angles, θ, the spin-0 and spin-1/2 cross-sections are identical. The effect of the magnetic scattering term $(-q^2/2M^2)\sin^2\theta/2$ becomes evident at large scattering angles; the spin-0 cross-section falls to zero as $\theta \to \pi$, while the spin-1/2 cross-section remains finite. The cross-section of the spin-1/2 target with the assumption of the dipole form factor is also shown in Figure 1.2.

1.2.1 Elastic Electron-Proton Scattering

Detailed study of the nucleons is very important to understand the nucleus. In the mid-1950s, a series of experiments led by Robert Hofstadter at Stanford University established electron scattering as a powerful technique for exploring nuclear structure [9–11]. In particular, this work established that the proton has an extended charge distribution and measured its size. One of the main advantages of this technique

is that it can reveal the electromagnetic structure of a nucleon or nucleus. The small cross-sections associated with electromagnetic processes necessitate a very high-luminosity experiment with intense electron beams. Despite this limitation, electron scattering or lepton scattering more generally is a precision probe of nuclear structure.

1.2.1.1 Born Approximation

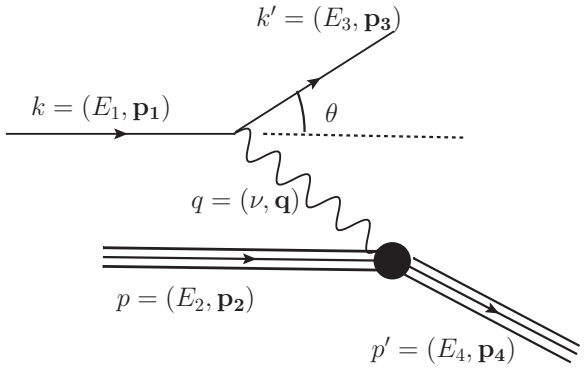

Figure 1.3. Leading order Feynman diagram for elastic electron-proton scattering in the one-photon exchange (Born) approximation.

The basic electron-proton scattering is the elastic scattering in the one-photon exchange (OPE) approximation [6]. That is, in the reaction $e^- + p \rightarrow e^- + p$, the stationary proton is probed by the electron by exchanging only one photon, while the struck nucleon stays in its ground state and the energy and momentum of the electron-nucleon system are conserved. If the proton is a point charge q with Dirac magnetic moment $q\hbar/2Mc$, one would have the same Equation (1.2.9) for the differential cross-section. But, in reality, the proton is not a point charge. It has an internal structure with quarks and gluons. Therefore, modifications are needed to the matrix element accordingly by keeping the electron tensor as is and addressing the proton tensor separately:

$$|\bar{M}|^2 = \frac{e^4}{q^4} L_e^{\mu\nu} W_{\mu\nu}^{proton} \tag{1.2.12}$$

The black solid circle in Figure 1.3 indicates that the QED vertex factor is to be modified to take into account the nucleon's internal electromagnetic structure. By applying the Feynman rules for QED, the invariant amplitude for elastic $e^- N$ scattering can be read from the diagram as,

$$-iM = \bar{u}(k')(ig_e\gamma^\mu)u(k)\left(-i\frac{g_{\mu\nu}}{q^2}\right)\bar{u}(p')(-ig_e\Gamma^\nu)u(p). \tag{1.2.13}$$

Here it is noted that one of the electron vertex factors, γ^μ from the lepton-lepton scattering in Equation (1.2.3), which represents scattering from a spin-1/2 point particle, is replaced by the nucleon vertex factor, or current Γ^ν, which describes a spin-1/2 composite proton. Its magnetic moment is determined by the combined spin and orbital angular momentum of three valence quarks, the surrounding sea of transient quark-antiquark pairs and gluons that fluctuate in and out of existence in the strong color field of the valence quarks. Therefore, the nucleon vertex factor Γ^ν in Equation (1.2.13) can be generalized as,

$$\Gamma_\mu = \gamma_\mu F_1(Q^2) + (iF_2(Q^2) + \tilde{F}_2(Q^2)\gamma_5)\sigma_{\mu\nu}q^\nu + \tilde{F}_3(Q^2)(q_\mu \not{q} - q^2\gamma_\mu)\gamma_5, \tag{1.2.14}$$

by noting that the electromagnetic current is conserved [12]. The objects $F_1, F_2, \tilde{F}_2, \tilde{F}_3$ are called *form factors*. These form factors are Lorentz invariant quantities which are the functions of $Q^2 = -q^2 = (p - p')^2$. Here is the summary of the physics of these form factors.

REFERENCES

[1] H. Geiger and E. Marsden. Proceedings of the Royal Society of London, Series A 82, 495 (1909).

[2] E. Rutherford. Philosophical Magazine, 21, 669-688 (1911).

[3] H. Geiger and E. Marsden. Philosophical Magazine, 25, 148 (1913).

[4] O. Stern. Nature, 132, 169 (1933).

[5] Francis Halzen and Alan D. Martin. Quark and Leptons: An Introductory Course in Modern Particle Physics. John Wiley and Sons, (1984).

[6] Michael E. Peskin and Daniel V. Schroeder. An Introduction to Quantum Field Theory. Westview Press, (1995).

[7] C. Amsler *et al.* (Particle Data Group), "2008 Review of Particle Physics". Phys. Lett. B 667, 1 (2008).

[8] M. Amaryan. Class notes, (2007).

[9] Robert Hofstadter and Robert W. McAllister. American Physical Society, Phys. Rev. 98, 217-218 (1955).

[10] Robert Hofstadter and Robert McAllister. Phys. Rev. 102, 851 (1956).

[11] Robert Hofstadter. Rev. of Mod. Phys. 28(3), 214 (1956).

[12] Amitabha Lahiri and Palash B. Pal. A First Book Of Quantum Field Theory. CRC Press, (2001).

VITA here